

Provably-Stable Neural Network-Based Control of Nonlinear Systems^{*}

Anran Li, John P. Swensen, Mehdi Hosseinzadeh^{*}

School of Mechanical and Materials Engineering, Washington State University, Pullman, WA 99164, USA

Abstract

In recent years, Neural Networks (NNs) have been employed to control nonlinear systems due to their potential capability in dealing with situations that might be difficult for conventional nonlinear control schemes. However, to the best of our knowledge, the current literature on NN-based control lacks theoretical guarantees for stability and tracking performance. This precludes the application of NN-based control schemes to systems where stringent stability and performance guarantees are required. To address this gap, this paper proposes a systematic and comprehensive methodology to design provably-stable NN-based control schemes for affine nonlinear systems. Rigorous analysis is provided to show that the proposed approach guarantees stability of the closed-loop system with the NN in the loop. Also, it is shown that the resulting NN-based control scheme ensures that system states asymptotically converge to a neighborhood around the desired equilibrium point, with a tunable proximity threshold. The proposed methodology is validated and evaluated via simulation studies on an inverted pendulum and experimental studies on a Parrot Bebop 2 drone.

Keywords: Neural network-based control, Stability guarantees, Performance analysis, Predictive control, Nonlinear systems

1. Introduction

Nonlinear systems appear in today's real-world control problems. Historically, nonlinear systems have been addressed through various techniques of linearization and application of well-established linear control system theory. Inherently, almost all physical systems are nonlinear and the foundational linear system theory incentivized methodologies and regimes where nonlinear systems could be treated as linear systems. For instance, one can use the feedback linearization technique [1, 2] to convert the nonlinear system into a linear system, and then use linear control techniques (see e.g., [3, 4]) to address the control problem. Another approach is to successively linearize the nonlinear system and use the Linear Quadratic Regulator (LQR) method to control

^{*}This research has been supported by WSU Voiland College of Engineering and Architecture through a start-up package to M. Hosseinzadeh.

^{*}Corresponding author.

Email addresses: anran.li@wsu.edu (Anran Li), john.swensen@wsu.edu (John P. Swensen), mehdi.hosseinzadeh@wsu.edu (Mehdi Hosseinzadeh)

the nonlinear system; this approach is called iterative LQR and has been widely studied in prior work, e.g., [5, 6, 7, 8, 9, 10, 11].

A different approach to control nonlinear systems is to deal with them directly by using nonlinear control techniques; see [1, 12, 13, 14] for details of some of existing techniques. One of the challenges in direct controlling of nonlinear systems is guaranteeing stability at all operating points [15, 16]. One possible approach to address this issue, which has gained growing attention [17, 18, 19, 20, 21], is to use Neural Networks (NN) in the control loop and in combination with Lyapunov theory.

In this context, [22] proposes a NN-based controller which provides a Lyapunov function for stability purposes; however, it does not address control objectives and performance metrics. Augmented neural Lyapunov control has been introduced in [23] to address the control problem; however, [23] does not provide theoretical analysis for stability and convergence. A combination of LQR and an online NN has been proposed in [24] to stabilize an inverted pendulum in upright posture, without providing guarantees on stability. In [25], a mixed H_2/H_∞ control has been integrated with a NN-based observer to reduce the uncertainty and to ensure the stability of unmanned aerial vehicles. Designing a Lyapunov-based nonlinear control determined from a NN has been discussed in [26], which uses the Lyapunov theory to compute the control law; note that online computations make this method inappropriate for real-time applications. A NN-based adaptive control has been proposed in [27] for affine nonlinear system, and theoretical guarantees are developed under the assumption that the NN's approximation error is very small. A stabilizing control law for personal aerial vehicles based on exponentially stabilizing control Lyapunov functions has been developed in [28] and [29], without providing a formal stability proof with the developed NN in the loop. Ref. [30] integrates optimization-based projection layers into a neural network-based policy to improve robustness and performance of the system; note that this method is limited to linear systems. A NN-based adaptive control has been proposed in [31], which is developed based upon the nonlinear dynamic inversion approach; note that this method cannot be applied to a wide range of systems and does not provide stability and convergence proofs. A NN-based Lyapunov-induced control law is developed in [32], which determines a control Lyapunov function for the system; since this method stops as soon as one control Lyapunov function is discovered, it can lead to a poor performance.

Despite being promising in academic experiments, many key challenges about using NNs in control loops remain unsolved, which prevent society from deploying such approaches widely. In particular, to the best of our knowledge, the current literature on NN-based control lacks theoretical guarantees for stability and performance. This paper aims at addressing this gap by introducing a new approach to provable NN-based control, where the controller we train with is co-developed so that it is amenable to the provable NN-based solution. First, this paper proposes a novel one-step-ahead predictive control scheme that determines the optimal control signal at any time instant, as well as a stabilizing Lyapunov function; stability and tracking properties of the proposed one-step-ahead predictive control scheme are theoretically proven by means of formal methods. This paper then discusses how to train a NN that mimics the behavior of the proposed one-step-ahead predictive control scheme. Also, it formally investigates stability and tracking properties of the closed-loop system when the trained NN is in the control loop, and characterizes the tracking error. Finally, this paper assesses the effectiveness of the proposed one-step-ahead predictive control scheme and the associated NN-based control scheme via extensive simulation studies on an inverted pendulum system and experimental results on a drone. Figure 1 presents the general structure of the proposed approach.

The key contributions of this paper are: i) developing a novel one-step-ahead predictive

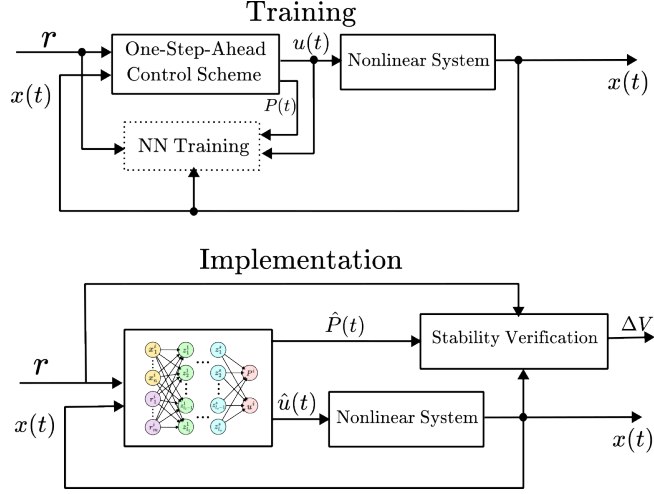


Figure 1: General structure of proposed methodology.

control scheme for nonlinear systems and analytically proving its theoretical properties; and ii) developing a NN-based control scheme for nonlinear systems, formally proving its stability and convergence properties, and evaluating the effectiveness of the proposed control schemes via simulation and experimental studies.

The main features of the propose NN-based control scheme compared with prior work are as follows. First, rather than considering a general Lyapunov function for the system, this paper learns a stabilizing quadratic Lyapunov function for each operating point, which is simpler and more straightforward; such a feature broadens the range of the control problems that can be addressed by the proposed NN-based control method. Second, this paper characterizes the degradation in the tracking performance due to learning process, and provides a single design parameter to manipulate the degradation; this feature allows the practitioners to obtain the desired tracking performance by adjusting a single parameter without concerning about the accuracy of the NN in imitating the desired control policy. Third, the developed NN-based control scheme imitates the optimal solution according to the given objective function; this feature allows the practitioners to incorporate any objective functions into the scheme without changing its structure. Fourth, this paper linearizes the nonlinear system at any time instant and determines a control signal based on the current operating point of the system; such a features allows us to apply the proposed NN-based control method (probably with some minor modification) to time-varying linear systems (we leave studying theoretical guarantees for such applications to future work). Fifth, running time of the developed NN-based control scheme is significantly smaller than that of the corresponding optimization-based scheme (our numerical analysis shows that using a NN that imitate the behavior of the one-step-ahead predictive control scheme can improve the computing efficiency by $\sim 319\%$); we believe that the proposed approach provides useful insights for future work on how to implement sophisticated and time-consuming control schemes despite limitations on available computing power, without hampering stability or significantly degrading the performance.

The rest of this paper is organized as follows. Section 2 states the problem. Section 3 presents details of the proposed one-step-ahead predictive control method and discusses its theoretical

properties. Section 4 reports the data collection and NN training procedures. The NN-based control scheme is introduced in Section 5 and its properties are proven analytically. Section 6 evaluates the proposed method via extensive simulation studies. Finally, Section 8 concludes the paper.

Notation. We denote the set of real numbers by \mathbb{R} , the set of positive real numbers by $\mathbb{R}_{>0}$, and the set of non-negative real numbers by $\mathbb{R}_{\geq 0}$. We use $\mathbb{Z}_{\geq 0}$ to denote the set of non-negative integer numbers. For a matrix A , $A > 0$ indicates that A is positive definite, and $A \geq 0$ indicates that A is positive semi-definite. We denote the transpose of matrix A by A^\top . Given $x \in \mathbb{R}^n$ and $Q \in \mathbb{R}^{n \times n}$, $\|x\|_Q = \sqrt{x^\top Q x}$. Given the set Ψ , $|\Psi|$ indicates its cardinality. For a function $Y(x)$, $Y(x)|_{x=x^\dagger}$ indicates that the function $Y(x)$ is evaluated at $x = x^\dagger$. We use I_n to denote $n \times n$ identity matrix.

2. Problem Statement

Consider the following discrete-time affine nonlinear system:

$$x(t+1) = f(x(t)) + g(x(t))u(t), \quad (1a)$$

$$y(t) = h(x(t), u(t)), \quad (1b)$$

where $x(t) = [x_1(t) \dots x_n(t)] \in \mathbb{R}^n$ is the state vector at time instant t , $u(t) = [u_1(t) \dots u_p(t)] \in \mathbb{R}^p$ is the control input at time instant t , $y(t) = [y_1(t) \dots y_m(t)] \in \mathbb{R}^m$ is the output vector at time instant t , and $f: \mathbb{R}^n \rightarrow \mathbb{R}^n$, $g: \mathbb{R}^n \rightarrow \mathbb{R}^{n \times p}$, and $h: \mathbb{R}^n \times \mathbb{R}^p \rightarrow \mathbb{R}^m$ are known nonlinear functions. Let $\mathcal{X} \subseteq \mathbb{R}^n$ be the operating region¹ of the system described in (1), i.e., $x(t) \in \mathcal{X}$, $\forall t \geq 0$.

Assumption 1. For any given $x^\dagger \in \mathcal{X}$, let $A^\dagger = \frac{\partial f(x)}{\partial x}|_{x=x^\dagger}$ and $B^\dagger = g(x^\dagger)$; then, the pair (A^\dagger, B^\dagger) is stabilizable. In other words, the linearized system around any point in the set \mathcal{X} is stabilizable.

Assumption 2. For any $x^\dagger \in \mathcal{X}$, we have $\|f(x^\dagger) - A^\dagger x^\dagger\| \leq \delta$, for some $\delta \in \mathbb{R}_{\geq 0}$, where $A^\dagger = \frac{\partial f(x)}{\partial x}|_{x=x^\dagger}$. In other words, the linearization error can be upper-bounded with δ throughout the operating region \mathcal{X} .

Assumption 3. Functions $f(x)$ and $g(x)$ are μ_f and μ_g Lipschitz continuous, respectively, throughout the operating region \mathcal{X} . That is, for any $x^\dagger \in \mathcal{X}$ and $x^\ddagger \in \mathcal{X}$, we have $\|f(x^\dagger) - f(x^\ddagger)\| \leq \mu_f \|x^\dagger - x^\ddagger\|$ and $\|g(x^\dagger) - g(x^\ddagger)\| \leq \mu_g \|x^\dagger - x^\ddagger\|$.

Let $r \in \mathbb{R}^m$ be the desired reference. Let \bar{x}_r and \bar{u}_r be the steady state and control input, respectively, such that

$$\bar{x}_r = f(\bar{x}_r) + g(\bar{x}_r)\bar{u}_r, \quad r = h(\bar{x}_r, \bar{u}_r), \quad (2)$$

where $\bar{x}_r \in \mathcal{X}$. Such a reference signal is called a steady-state admissible reference; we denote the set of all steady-state admissible references by $\mathcal{R} \subseteq \mathbb{R}^m$.

This paper addresses the following problem.

Problem 1. For any given $r \in \mathcal{R}$, design a NN-based control scheme that determines the optimal control input to steer the state of system (1) to \bar{x}_r and its steady input to \bar{u}_r .

¹Note that this paper does not aim at enforcing the operating region as a constraint. Indeed, we will utilize the set \mathcal{X} to determine the region of attraction of the proposed methods. Future work will discuss how to extend the proposed methods to guarantee state and input constraint satisfaction at all times.

3. One-Step-Ahead Predictive Control

Problem 1 is a well-known problem in the literature and several methods have been presented to address it (see, e.g., [22, 28, 31]). However, to the best of our knowledge, the current literature does not guarantee stability and convergence in the presence of training errors in an analytic manner. Also, prior work focuses on providing a stabilizing control input, without discussing optimality of the obtained solution.

To address Problem 1, this section proposes a novel one-step-ahead predictive control scheme that determines the optimal control input and a quadratic stabilizing Lyapunov function depending on the current states of the system. The procedure of training a NN that imitates the behavior of the developed one-step-ahead predictive control will be reported in Section 4. Finally, Section 5 will develop a NN-based control scheme and will study its properties.

3.1. Control Structure

One possible approach to control system (1) is to utilize the Model Predictive Control (MPC) framework [33, 34], which determines the control input by solving a receding horizon optimal control problem. While resulting problems are convex for linear systems, they are not necessarily convex for nonlinear systems [13, 35], which creates challenges for stability proofs [36] and real-time implementations [37]. One possible approach to address the above-mentioned issues is to iteratively linearize the nonlinear system and use MPC for linear systems. It is well-known that [38, 39] when the prediction horizon is large, prediction errors due to linearization (and to model uncertainty and external disturbances) can significantly degrade the performance of the system and can even lead to instability. Prior work (e.g., [40]) suggests using one step ahead prediction to compute the control input at each time instant so as to bring the system states at the next time instant to a desired value. This subsection proposes a novel one-step-ahead predictive control for system (1), and investigates its stability and convergence properties. Once again, this paper does not aim at enforcing constraints on states and control inputs.

Given the desired reference $r \in \mathcal{R}$ and the current state $x(t)$, we determine the optimal control input $u^*(t) \in \mathbb{R}^p$ and the optimal Lyapunov matrix $P^*(t) \in \mathbb{R}^{n \times n}$ by solving the following optimization problem:

$$u^*(t), P^*(t) = \arg \min_{u, P} \|x^+ - \bar{x}_r\|_{Q_x}^2 + \|u - \bar{u}_r\|_{Q_u}^2 + V(x(t), r, P)^2, \quad (3a)$$

subject to the following constraints:

$$x^+ = A_t x(t) + B_t u, \quad (3b)$$

$$P > 0, \quad (3c)$$

$$V(x^+, r, P) - V(x(t), r, P) \leq -\theta \|x(t) - \bar{x}_r\|, \quad (3d)$$

where A_t and B_t describe the linearized system around the current state $x(t)$ (see Assumption 1), $\theta \in \mathbb{R}_{>0}$ is a design parameter, $V(x, r, P) := \|x - \bar{x}_r\|_P = \sqrt{[(x - \bar{x}_r)^\top P (x - \bar{x}_r)]}$ is the Lyapunov function², x^+ is the one-step-ahead prediction computed based on the linearized model around $x(t)$, and $Q_x = Q_x^\top \geq 0$ ($Q_x \in \mathbb{R}^{n \times n}$) and $Q_u = Q_u^\top > 0$ ($Q_u \in \mathbb{R}^{p \times p}$) are weighting matrices.

²For any r and $P > 0$, the function $V(x, r, P) := \|x - \bar{x}_r\|_P$ satisfies the Lyapunov conditions, i.e., i) $V(x, r, P) \geq 0$ for all x ; ii) $V(x, r, P) = 0$ if and only if $x = \bar{x}_r$; and iii) $V(x, r, P) \rightarrow \infty$ if $\|x\| \rightarrow \infty$.

The first and second terms in the cost function (3a) penalizes deviation from the desired steady state \bar{x}_r and steady input \bar{u}_r , respectively. The last term in cost function (3a) penalizes the Lyapunov function $V(x)$ (note that the main advantage of this term will be shown later). Constraint (3b) enforces the linearized dynamics, constraint (3c) enforces positive definiteness of the Lyapunov matrix P , and constraint (3d) indicates that the obtained control input must be stabilizing at the current time instant t .

Remark 1. Let system (1) be linear, i.e., $x(t+1) = Ax(t) + Bu(t)$. In this case, it is well-known that one can determine a single constant Lyapunov matrix $P > 0$. It can be shown that if the matrix P satisfies $\sqrt{\lambda_{\min}(P)} > \theta$, where $\lambda_{\min}(P)$ indicates the smallest eigenvalue of P , constraint (3d) imposes exponential stability (see [41] for the definition of exponential stability in discrete-time linear systems).

Remark 2. Let system (1) be linear, i.e., $x(t+1) = Ax(t) + Bu(t)$. In this case, the finite-time LQR control law with prediction horizon of one to steer the states of the system to \bar{x}_r can be obtained by solving the following optimization problem:

$$u^*(t) = \arg \min_u \|x(t) - \bar{x}_r\|_{R_x}^2 + \|u - \bar{u}_r\|_{R_u}^2 + \|x(t+1) - \bar{x}_r\|_{R_f}^2, \quad (4)$$

where $R_x = R_x^T > 0$ ($R_x \in \mathbb{R}^{n \times n}$), $R_u = R_u^T > 0$ ($R_u \in \mathbb{R}^{p \times p}$), and $R_f = R_f^T \geq 0$ ($R_f \in \mathbb{R}^{n \times n}$). Comparing (3) with (4) yields that, in the case of a linear system, the proposed one-step-ahead predictive control scheme provides the finite-time LQR control law with prediction horizon of one, where the weighting matrices are $R_x = P$, $R_u = Q_u$, and $R_f = Q_x$.

Remark 3. Although this paper considers one step ahead prediction in the cost function (3a), it is possible to extend the obtained results to problems with larger prediction horizon. In particular, it is possible to consider an infinite-horizon prediction horizon in (3a), as $\sum_{k=1}^{\infty} \|\hat{x}(k) - \bar{x}_r\|_{Q_x}^2 + \sum_{k=0}^{\infty} \|u(k) - \bar{u}_r\|_{Q_u}^2 + V(x(t), r, P)^2$, where $\hat{x}(k+1) = A\hat{x}(k) + Bu(k)$ with $\hat{x}(0) = x(t)$, is the predicted state vector based on the linearized model. Such a cost function resembles the iterative LQR with infinite horizon; see, e.g., [5, 6]. Note that, when the linearization error δ as in Assumption 2 is large, or the system is subject to model uncertainty and/or external disturbances, considering a large prediction horizon can significantly degrade the performance, and thus it is undesired.

3.2. Theoretical Analysis

This section studies theoretical properties of the proposed one-step-ahead predictive control scheme. First, we study the recursive feasibility of the proposed scheme.

Theorem 1 (Recursive Feasibility). Consider system (1) and suppose that (3) is feasible at $t = 0$. Then, it remains feasible for all $t > 0$.

Proof. Under Assumption 1, it is possible to determine a control input such that the dynamics of the linearized system around any point in the operating region \mathcal{X} is stable. Thus, no further effort is required to show that if $x(t) \in \mathcal{X}$, the optimization problem (3) is feasible; this completes the proof. \square

Next, we study the stability and convergence of the one-step-ahead predictive control scheme given in (3).

Theorem 2 (Stability and Convergence). *Consider system (1) and suppose that the control scheme described in (3) is used to control it. Then, for any given $r \in \mathcal{R}$, the tracking error $\|x(t) - \bar{x}_r\|$ remains bounded, and there exists $\sigma \in \mathbb{R}_{>0}$ such that $\|x(t) - \bar{x}_r\| \leq \sigma$ as $t \rightarrow \infty$.*

Proof. Let $(u^*(t), P^*(t))$ and $(u^*(t+1), P^*(t+1))$ be the optimal solutions at time instants t and $t+1$, respectively. To prove this theorem, we only need to show that $\Delta V(t) := V(x(t+1), r, P^*(t+1)) - V(x(t), r, P^*(t)) < 0$ whenever $\|x(t) - \bar{x}_r\| > \sigma$ for some $\sigma \in \mathbb{R}_{\geq 0}$.

We have:

$$\begin{aligned} \Delta V(t) &= \|x(t+1) - \bar{x}_r\|_{P^*(t+1)} - \|x(t) - \bar{x}_r\|_{P^*(t)} \\ &= \|f(x(t)) + g(x(t))u^*(t) - \bar{x}_r\|_{P^*(t+1)} - \|x(t) - \bar{x}_r\|_{P^*(t)}, \end{aligned} \quad (5)$$

We add and subtract the term $A_t x(t)$ from the first norm in the right-hand side of (5), where A_t representing the linearized dynamics at time instant t (see Assumption 1). Thus, according to triangle inequality³, we have:

$$\Delta V(t) \leq \|f(x(t)) - A_t x(t)\|_{P^*(t+1)} + \|A_t x(t) + g(x(t))u^*(t) - \bar{x}_r\|_{P^*(t+1)} - \|x(t) - \bar{x}_r\|_{P^*(t)}, \quad (6)$$

which according to Assumption 2 implies that⁴:

$$\Delta V(t) \leq \sqrt{\lambda_{\max}(P^*(t+1))}\delta - \|x(t) - \bar{x}_r\|_{P^*(t)} + \|A_t x(t) + g(x(t))u^*(t) - \bar{x}_r\|_{P^*(t+1)}, \quad (7)$$

where $\lambda_{\max}(P^*(t+1)) \in \mathbb{R}_{>0}$ is the maximum eigenvalue of matrix $P^*(t+1)$.

Adding and subtracting the term $\|A_t x(t) + g(x(t))u^*(t) - \bar{x}_r\|_{P^*(t)}$ to the right-hand side of the inequality (7) yields:

$$\begin{aligned} \Delta V(t) &\leq \sqrt{\lambda_{\max}(P^*(t+1))}\delta - \|x(t) - \bar{x}_r\|_{P^*(t)} + \|A_t x(t) + g(x(t))u^*(t) - \bar{x}_r\|_{P^*(t+1)} \\ &\quad - \|A_t x(t) + g(x(t))u^*(t) - \bar{x}_r\|_{P^*(t)} + \|A_t x(t) + g(x(t))u^*(t) - \bar{x}_r\|_{P^*(t)}, \end{aligned} \quad (8)$$

which according to the fact that $\|A_t x(t) + g(x(t))u^*(t) - \bar{x}_r\|_{P^*(t)} - \|x(t) - \bar{x}_r\|_{P^*(t)} \leq -\theta \|x(t) - \bar{x}_r\|$ (this is a direct implication from the optimization problem (3)) implies that:

$$\begin{aligned} \Delta V(t) &\leq \sqrt{\lambda_{\max}(P^*(t+1))}\delta - \theta \|x(t) - \bar{x}_r\| + \|A_t x(t) + g(x(t))u^*(t) - \bar{x}_r\|_{P^*(t+1)} \\ &\quad - \|A_t x(t) + g(x(t))u^*(t) - \bar{x}_r\|_{P^*(t)}. \end{aligned} \quad (9)$$

Let $J(u(t), P(t)|x(t), r)$ and $J(u(t+1), P(t+1)|x(t+1), r)$ be the cost of the control scheme given in (3) at time instants t and $t+1$, respectively. According to the optimality of the solution $(u^*(t+1), P^*(t+1))$ at time instant $t+1$, we have:

$$J(u^*(t+1), P^*(t+1)|x(t+1), r) \leq J(u^*(t), P^*(t)|x(t+1), r), \quad (10)$$

³Given $z_1, z_2 \in \mathbb{R}^n$ and $Q > 0$ ($Q \in \mathbb{R}^{n \times n}$), we have $\|z_1 + z_2\|_Q^2 = z_1^\top Q^{\frac{1}{2}} Q^{\frac{1}{2}} z_1 + z_2^\top Q^{\frac{1}{2}} Q^{\frac{1}{2}} z_2 + 2z_1^\top Q^{\frac{1}{2}} Q^{\frac{1}{2}} z_2 \leq \|Q^{\frac{1}{2}} z_1\|^2 + \|Q^{\frac{1}{2}} z_2\|^2 + 2\|Q^{\frac{1}{2}} z_1\| \|Q^{\frac{1}{2}} z_2\|$, which implies that $\|z_1 + z_2\|_Q^2 \leq (\|Q^{\frac{1}{2}} z_1\| + \|Q^{\frac{1}{2}} z_2\|)^2$, or $\|z_1 + z_2\|_Q^2 \leq (\|z_1\|_Q + \|z_2\|_Q)^2$. Thus, we have $\|z_1 + z_2\|_Q \leq \|z_1\|_Q + \|z_2\|_Q$.

⁴Given $z \in \mathbb{R}^n$ and $Q > 0$ ($Q \in \mathbb{R}^{n \times n}$), we have $\lambda_{\min}(Q) \|z\|^2 \leq \|z\|_Q^2 \leq \lambda_{\max}(Q) \|z\|^2$, which implies that $\sqrt{\lambda_{\min}(Q)} \|z\| \leq \|z\|_Q \leq \sqrt{\lambda_{\max}(Q)} \|z\|$.

which implies that

$$\begin{aligned} & \|A_{t+1}x(t+1) + B_{t+1}u^*(t+1) - \bar{x}_r\|_{Q_x}^2 + \|u^*(t+1) - \bar{u}_r\|_{Q_u}^2 + \|x(t+1) - \bar{x}_r\|_{P^*(t+1)}^2 \\ & \leq \|A_{t+1}x(t+1) + B_{t+1}u^*(t+1) - \bar{x}_r\|_{Q_x}^2 + \|u^*(t+1) - \bar{u}_r\|_{Q_u}^2 + \|x(t+1) - \bar{x}_r\|_{P^*(t)}^2. \end{aligned} \quad (11)$$

Thus, we have:

$$\|x(t+1) - \bar{x}_r\|_{P^*(t+1)}^2 \leq \|x(t+1) - \bar{x}_r\|_{P^*(t)}^2. \quad (12)$$

or

$$\|x(t+1) - \bar{x}_r\|_{P^*(t+1)} \leq \|x(t+1) - \bar{x}_r\|_{P^*(t)}. \quad (13)$$

Replacing $x(t+1)$ with $f(x(t)) + g(x(t))u^*(t)$ in (13), and adding and subtracting $A_t x(t)$, it follows from (13) that⁵:

$$\begin{aligned} & \|A_t x(t) + g(x(t))u^*(t) - \bar{x}_r\|_{P^*(t+1)} \leq \\ & \|f(x(t)) - A_t x(t)\|_{P^*(t+1)} + \|f(x(t)) - A_t x(t)\|_{P^*(t)} + \|A_t x(t) + g(x(t))u^*(t) - \bar{x}_r\|_{P^*(t)} \leq \\ & \sqrt{\lambda_{\max}(P^*(t+1))}\delta + \sqrt{\lambda_{\max}(P^*(t))}\delta + \|A_t x(t) + g(x(t))u^*(t) - \bar{x}_r\|_{P^*(t)}. \end{aligned} \quad (14)$$

Thus, according to (9) and (14), we have:

$$\Delta V(t) \leq 2\sqrt{\lambda_{\max}(P^*(t+1))}\delta + \sqrt{\lambda_{\max}(P^*(t))}\delta - \theta \|x(t) - \bar{x}_r\|. \quad (15)$$

Setting $\sigma = \frac{3\sqrt{\bar{\lambda}_P}\delta}{\theta}$, where $\bar{\lambda}_P = \sup_{t \geq 0} \lambda_{\max}(P^*(t))$ ($\bar{\lambda}_P \in \mathbb{R}_{>0}$), no further effort is needed to complete the proof. \square

Remark 4. Since θ is a design parameter, the upper-bound of the tracking error (i.e., σ) can be made arbitrarily small. However, our numerical experiments show that the optimization problem (3) can become numerically ill-conditioned for large values of θ . Future work will provide techniques to mitigate numerical issues in the proposed methodology.

Remark 5. It is obvious that for linear systems, since $\delta = 0$, the equilibrium point \bar{x}_r is asymptotically stable with the proposed one-step-ahead predictive control given in (3).

Remark 6. Theorem 2 indicates that, despite the conventional nonlinear control methods, one can manipulate the achieved tracking error by adjusting only one scalar in the proposed one-step-ahead predictive control given in (3).

4. Data Collection and NN Training

At any time instant t , the proposed one-step-ahead predictive control receives the desired reference r and the current state vector $x(t)$, and solves the optimization problem (3) to compute the control input $u(t)$ and the Lyapunov matrix $P(t)$. However, solving the optimization problem (3) can be computationally challenging, and may not be realistic for real-time applications.

⁵Given $z_1, z_2 \in \mathbb{R}^n$ and $Q > 0$ ($Q \in \mathbb{R}^{n \times n}$), following the arguments similar to footnote 3, it can be shown that $\|z_1\|_Q - \|z_2\|_Q \leq \|z_1 + z_2\|_Q \leq \|z_1\|_Q + \|z_2\|_Q$.

To address this issue, we propose to train a NN to approximate the relationship between input parameters of the optimization problem (3) (i.e., state vector $x(t)$ and desired reference r) and output parameters of the optimization problem (3) (i.e., control input $u(t)$ and Lyapunov matrix $P(t)$), and use it in the loop to control system (1). Our intuition is that using the NN significantly decreases the computational burden of the proposed control scheme, as it reduces the problem of computing $u(t)$ and $P(t)$ into simple function evaluations. To do so, this section discusses the data collection and training procedure to train a NN that imitates the behavior of the one-step-ahead predictive control scheme developed in Section 3 in the operating region \mathcal{X} . Section 5 will investigate the theoretical properties of the closed-loop system with the NN in the loop in the presence of NN's approximation errors.

To obtain the training dataset, first, we divide the operating region \mathcal{X} and the set of steady-state admissible references \mathcal{R} into N_x and N_r grid cells, respectively; this process generates $N_x \cdot N_r$ data points which are denoted by (x^i, r^i) , $i = 1, \dots, N_x \cdot N_r$, where $x^i \in \mathcal{X}$ and $r^i \in \mathcal{R}$. Then, for each data point (x^i, r^i) , we solve the optimization problem (3) under the assumption that $x(t) = x^i$; this yields the optimal control input (denoted by u^i) and optimal Lyapunov matrix (denoted by P^i) for the data point (x^i, r^i) . Finally, the training dataset can be constructed as follows:

$$\mathbb{D}_{training} = \left\{ (x^i, r^i, u^i, P^i), i = 1 \dots, N_x \cdot N_r \right\}, \quad (16)$$

where the tuple (x^i, r^i, u^i, P^i) is the i th training data point. It is obvious that $|\mathbb{D}_{training}| = N_x \cdot N_r$. Note that one can use a larger N_x and N_r (i.e., divide the sets \mathcal{X} and \mathcal{R} into smaller cells) to make sure that enough training data is collected and the training dataset $\mathbb{D}_{training}$ covers all relevant aspects of the problem domain. Thus, the NN can be trained offline and there is no need for online adjustments to the network's parameters.

Once the training dataset $\mathbb{D}_{training}$ is collected, we use them to train a (deep) feedforward NN [42]. Feedforward NNs are flexible and scalable, and can be used to approximate complex relationships between input and out parameters; also, their training is relatively straightforward compared to other structures [43]. Figure 2 presents the general structure of the considered NN, where x^i and r^i are the inputs of the NN and u^i and P^i are its outputs. Note that although we do not claim to be optimal, our experiments suggest that a feedforward NN provides satisfactory performance. We use the growing method (see, e.g., [44, 45, 46]) to determine the number of hidden layers and neurons; that is, we start with a small network and increase the complexity until the desired accuracy is achieved. Note that we apply the dropout method [47, 48, 49, 50] to avoid overfitting. Also, to improve the training process, we use the cosine annealing strategy [51, 52] to adjust the learning rate. To evaluate the network's convergence, we use the mean squared error (MSE) loss function; see more details about the role of loss function in, e.g., [43].

5. NN-Based Control

Let a NN be trained as discussed in Section 4 to imitate the behavior of the one-step-ahead predictive control scheme described in Section 3. At each time instant t , let $\hat{u}(t) = u^*(t) + \Delta u(t)$ and $\hat{P}(t) = P^*(t) + \Delta P(t)$ be the output of the NN, where $\Delta u(t)$ and $\Delta P(t)$ indicate the difference between the optimal solutions and the NN outputs. Note that $\hat{P}(t)$ is not necessarily positive definite. We reasonably assume that [22] the NN functions satisfy the bounded condition for all states in the operating region \mathcal{X} ; this implies that $\Delta u(t)$ and $\Delta P(t)$ are bounded at any time instant t . We let $\bar{\Delta}u = \sup_{t \geq 0} \|\Delta u(t)\|$ and $\bar{\Delta}P = \sup_{t \geq 0} \|\Delta P(t)\|$, where $\bar{\Delta}u, \bar{\Delta}P \in \mathbb{R}_{\geq 0}$.

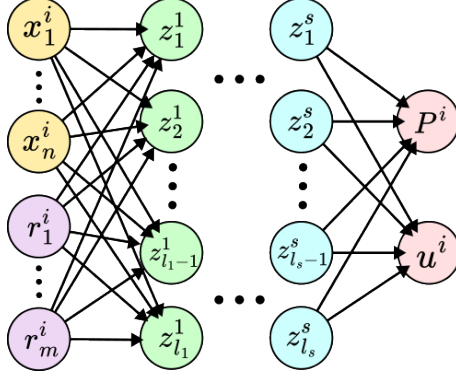


Figure 2: The NN trained to approximate the solution of (3), with s hidden layers and l_i neurons in the i th hidden layer.

5.1. Theoretical Analysis

The following theorem shows that if the trained NN is utilized in the loop to control system (1), the system is stable and the tracking error remains bounded. See Figure1 for the general structure of the proposed NN-based control scheme.

Theorem 3. Consider system (1), and suppose that a NN trained to imitate the behavior of the control scheme (3) is utilized in the control loop. Let $r \in \mathcal{R}$ be the desired reference signal. Then, for sufficiently large θ , the tracking error $\|x(t) - \bar{x}_r\|$ remains bounded, and there exists $\vartheta \in \mathbb{R}_{>0}$ such that $\|x(t) - \bar{x}_r\| \leq \vartheta$ as $t \rightarrow \infty$.

Proof. Let $\Delta V(t) := V(x(t+1), r, \hat{P}(t+1)) - V(x(t), r, \hat{P}(t))$. We have:

$$\begin{aligned} \Delta V(t) &= \|x(t+1) - \bar{x}_r\|_{P^*(t+1)+\Delta P(t+1)} - \|x(t) - \bar{x}_r\|_{P^*(t)+\Delta P(t)} \\ &= \|f(x(t)) + g(x(t))u^*(t) + \Delta u(t) - \bar{x}_r\|_{P^*(t+1)+\Delta P(t+1)} - \|x(t) - \bar{x}_r\|_{P^*(t)+\Delta P(t)}. \end{aligned} \quad (17)$$

According to triangle inequality (see footnote 3), Equation (17) can be rewritten as:

$$\begin{aligned} \Delta V(t) &\leq \|f(x(t)) + g(x(t))u^*(t) - \bar{x}_r\|_{P^*(t+1)+\Delta P(t+1)} + \|g(x(t))\Delta u(t)\|_{P^*(t+1)+\Delta P(t+1)} \\ &\quad - \|x(t) - \bar{x}_r\|_{P^*(t)+\Delta P(t)}, \end{aligned} \quad (18)$$

which implies that⁶:

$$\begin{aligned} \Delta V(t) &\leq \|f(x(t)) + g(x(t))u^*(t) - \bar{x}_r\|_{P^*(t+1)} + \sqrt{\Delta P} \|f(x(t)) + g(x(t))u^*(t) - \bar{x}_r\| \\ &\quad + \|g(x(t))\Delta u(t)\|_{P^*(t+1)+\Delta P(t+1)} - \|x(t) - \bar{x}_r\|_{P^*(t)} + \sqrt{\Delta P} \|x(t) - \bar{x}_r\|. \end{aligned} \quad (19)$$

According to Theorem 2, it follows from (19) that:

$$\begin{aligned} \Delta V(t) &\leq 3\sqrt{\lambda_P}\delta - \theta \|x(t) - \bar{x}_r\| + \sqrt{\Delta P} \|x(t) - \bar{x}_r\| + \|g(x(t))\Delta u(t)\|_{P^*(t+1)+\Delta P(t+1)} \\ &\quad + \sqrt{\Delta P} \|f(x(t)) + g(x(t))u^*(t) - \bar{x}_r\|. \end{aligned} \quad (20)$$

At this stage, we upper bound the fourth and fifth terms in (20) as follows:

⁶Given $z \in \mathbb{R}^n$ and $Q_1, Q_2 \in \mathbb{R}^{n \times n}$, let $\|z\|_{Q_1} = \sqrt{z^T Q_1 z}$, $\|z\|_{Q_2} = \sqrt{z^T Q_2 z}$, and $\|z\|_{Q_1+Q_2} = \sqrt{z^T (Q_1 + Q_2) z}$. Thus, it can be easily shown that $\|z\|_{Q_1} - \|z\|_{Q_2} \leq \|z\|_{Q_1+Q_2} \leq \|z\|_{Q_1} + \|z\|_{Q_2}$. Also, $\|z\|_{Q_1} \leq \sqrt{\|Q_1\|} \|z\|$ and $\|z\|_{Q_2} \leq \sqrt{\|Q_2\|} \|z\|$.

- Fourth Term: This term can be upper bounded as (see footnote 6):

$$\begin{aligned} \|g(x(t)) \Delta u(t)\|_{P^*(t+1)+\Delta P(t+1)} &\leq \|g(x(t)) \Delta u(t)\|_{P^*(t+1)} + \|g(x(t)) \Delta u(t)\|_{\Delta P(t+1)} \\ &\leq \left(\sqrt{\bar{\lambda}_p} + \sqrt{\bar{\Delta P}}\right) \|g(x(t)) \Delta u(t)\|. \end{aligned} \quad (21)$$

By adding and subtracting $g(\bar{x}_r) \Delta u(t)$ in the norm of right-hand side, and using the Cauchy–Schwarz inequality and triangle inequality, it follows from (21) that:

$$\begin{aligned} \|g(x(t)) \Delta u(t)\|_{P^*(t+1)+\Delta P(t+1)} &\leq (\sqrt{\bar{\lambda}_p} + \sqrt{\bar{\Delta P}}) \|g(x(t)) - g(\bar{x}_r)\| \|\Delta u(t)\| \\ &\quad + (\sqrt{\bar{\lambda}_p} + \sqrt{\bar{\Delta P}}) \|g(\bar{x}_r)\| \|\Delta u(t)\|. \end{aligned} \quad (22)$$

Finally, according to Assumption 3, inequality 22 can be expressed as:

$$\|g(x(t)) \Delta u(t)\|_{P^*(t+1)+\Delta P(t+1)} \leq (\sqrt{\bar{\lambda}_p} + \sqrt{\bar{\Delta P}}) \mu_g \Delta \bar{u} \|x(t) - \bar{x}_r\| + (\sqrt{\bar{\lambda}_p} + \sqrt{\bar{\Delta P}}) \|g(\bar{x}_r)\| \Delta \bar{u}. \quad (23)$$

Note that for any given $r \in \mathcal{R}$, $\|g(\bar{x}_r)\|$ is bounded.

- Fifth Term: By adding and subtracting $A_t x(t)$ and according to Assumption 2 and triangle inequality, we have:

$$\sqrt{\bar{\Delta P}} \|f(x(t)) + g(x(t)) u^*(t) - \bar{x}_r\| \leq \sqrt{\bar{\Delta P}} \delta + \sqrt{\bar{\Delta P}} \|A_t x(t) + g(x(t)) u^*(t) - \bar{x}_r\|. \quad (24)$$

At any time instant t , optimization problem (3) ensures that $\|A_t x(t) + g(x(t)) u^*(t) - \bar{x}_r\|_{P^*(t)} \leq \|x(t) - \bar{x}_r\|_{P^*(t)}$. Thus, according to footnote 4, we have:

$$\sqrt{\bar{\lambda}_p} \|A_t x(t) + g(x(t)) u^*(t) - \bar{x}_r\| \leq \sqrt{\bar{\lambda}_p} \|x(t) - \bar{x}_r\|, \quad (25)$$

where $\bar{\lambda}_p := \inf_{t \geq 0} \lambda_{\min}(P^*(t))$ ($\bar{\lambda}_p \in \mathbb{R}_{>0}$), with $\lambda_{\min}(P^*(t))$ being the smallest eigenvalue of matrix $P^*(t)$, and $\bar{\lambda}_p$ is defined in the proof of Theorem 2. Thus, according to (25), it follows from (23) that:

$$\sqrt{\bar{\Delta P}} \|f(x(t)) + g(x(t)) u^*(t) - \bar{x}_r\| \leq \sqrt{\bar{\Delta P}} \delta + \sqrt{\bar{\Delta P}} \frac{\sqrt{\bar{\lambda}_p}}{\sqrt{\bar{\lambda}_p}} \|x(t) - \bar{x}_r\|. \quad (26)$$

Finally, combining (20), (23), and (26) yields:

$$\begin{aligned} \Delta V(t) &\leq 3\sqrt{\bar{\lambda}_p} \delta + \sqrt{\bar{\Delta P}} \delta + (\sqrt{\bar{\lambda}_p} + \sqrt{\bar{\Delta P}}) \|g(\bar{x}_r)\| \Delta \bar{u} \\ &\quad - \left(\theta - \sqrt{\bar{\Delta P}} - \frac{\sqrt{\bar{\Delta P}} \sqrt{\bar{\lambda}_p}}{\sqrt{\bar{\lambda}_p}} - (\sqrt{\bar{\lambda}_p} + \sqrt{\bar{\Delta P}}) \mu_g \Delta \bar{u} \right) \|x(t) - \bar{x}_r\|, \end{aligned} \quad (27)$$

which completes the proof by selecting $\theta > \sqrt{\Delta P} + \frac{\sqrt{\Delta P}\sqrt{\lambda_p}}{\sqrt{\lambda_p}} + (\sqrt{\lambda_p} + \sqrt{\Delta P})\mu_g\Delta\bar{u}$, and setting ϑ as follows:

$$\vartheta = \frac{3\sqrt{\lambda_p}\delta + \sqrt{\Delta P}\delta + (\sqrt{\lambda_p} + \sqrt{\Delta P})\|g(\bar{x}_r)\|\Delta\bar{u}}{\theta - \sqrt{\Delta P} - \frac{\sqrt{\Delta P}\sqrt{\lambda_p}}{\sqrt{\lambda_p}} - (\sqrt{\lambda_p} + \sqrt{\Delta P})\mu_g\Delta\bar{u}}. \quad (28)$$

□

Remark 7. Since θ is a design parameter, the upper-bound of the tracking error when a NN is in the control loop (i.e., ϑ given in (28)) can be made arbitrarily small.

Remark 8. According to (28), in the presence of an ideal NN (i.e., $\Delta\bar{u} = \Delta P = 0$), the properties of the main controller (i.e., properties discussed in Theorem 2) are recovered, i.e., $\vartheta = \sigma$.

5.2. Region of Attraction

The proposed one-step-ahead predictive control given in (3) and the NN-based control described in Section 4 are developed such that the stability of system (1) is guaranteed in the operating region \mathcal{X} . However, they do not guarantee that the trajectory of the system remains in the operating region \mathcal{X} at all times. Thus, it is important to determine the Region of Attraction (RoA) of the proposed methods.

For any steady-state admissible reference r , the RoA is defined as the set of all initial conditions belonging to the set \mathcal{X} such that ensued trajectory remains inside the set \mathcal{X} . In mathematical terms, for a given $r \in \mathcal{R}$, the RoA $\Phi(r) \subseteq \mathcal{X}$ including \bar{x}_r can be defined as:

$$\Phi(r) = \{x \in \mathcal{X} | \hat{x}(k|x, r) \in \mathcal{X}, k \in \mathbb{Z}_{\geq 0}\}, \quad (29)$$

where $\hat{x}(k|x, r)$ is the predicted state from the initial state x at the prediction instant k , when the desired reference is r , and the one-step-ahead predictive scheme (3) or the NN-based scheme described in Section 5 are employed to control system 1.

The most intuitive way to estimate the set $\Phi(r)$ is described below. First, divide the set \mathcal{R} into $n_{\mathcal{R}}$ non-overlapping regions \mathcal{R}_i , $i \in \{1, \dots, n_{\mathcal{R}}\}$; this can be done by using existing techniques, e.g., Delaunay tessellation [53, 54]. Then, for each region \mathcal{R}_i , start with a large set $\Phi(r)$ (usually the set \mathcal{X}) including the set of steady-state admissible equilibria associated with the region \mathcal{R}_i (i.e., $\bar{\mathcal{R}}_i = \{x | \exists r \in \mathcal{R}_i \text{ such that } x = \bar{x}_r\}$), and compute simulated trajectories to find a $\tilde{x} \in \mathcal{X}$ and $\tilde{r} \in \mathcal{R}_i$ such that $\hat{x}(t|\tilde{x}, \tilde{r}) \notin \mathcal{X}$ at some t ; see Figure3 for a geometric illustration. If such a point is found, the set $\Phi(r)$ is falsified and should be shrunk by excluding a neighbourhood around \tilde{x} . This falsification procedure should be computed until all simulated trajectories remain in \mathcal{X} at all times. Note that although the above-mentioned procedure can be expensive from the computational viewpoint, it should be performed only at design-time and does not require human intervention.

6. Simulation Results

This section assesses the effectiveness of the proposed methodology on an inverted pendulum system; see Figure4. The dynamics of the system can be described as [55]:

$$mL^2\ddot{\alpha} = mgL \sin \alpha + \tau, \quad (30)$$

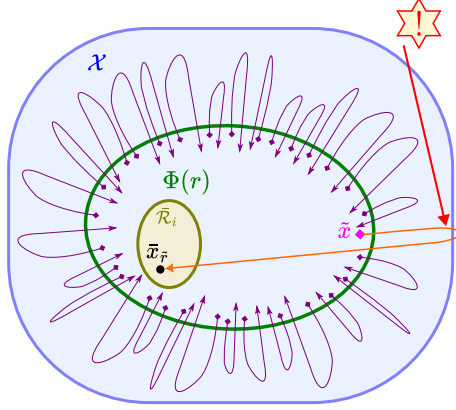


Figure 3: Geometric illustration of the falsification procedure for determining the RoA $\Phi(r)$.

where α represents angle of the inverted pendulum, τ is the torque generated from a motor rotating the pendulum, and $m = 1$ [kg] and $L = 1$ [m] are the pendulum mass and the distance from the center of mass, respectively. We assume that $\mathcal{X} = [-5, 5] \times [-5, 5]$ and $\mathcal{R} = [-1, 1]$. The state-space representation for this system is:

$$\dot{x}_1 = x_2, \quad (31a)$$

$$\dot{x}_2 = g \sin(x_1) + \tau, \quad (31b)$$

where $x_1 = \alpha$ and $x_2 = \dot{\alpha}$. We use Euler's method to discretize system (30) with the sampling period of $\Delta T = 0.1$ seconds, i.e.,

$$x_1(t+1) = x_1(t) + \Delta T \cdot x_2(t), \quad (32a)$$

$$x_2(t+1) = x_2(t) + \Delta T \cdot g \cdot \sin(x_1(t)) + \Delta T \cdot \tau(t), \quad (32b)$$

We use the proposed NN-based scheme to control system (32). First, we grid the above-mentioned sets \mathcal{X} and \mathcal{R} with steps of 0.1 to generate 200,000 data points. Then, we use YALMIP [56] to solve the optimization problem (3) with $Q_x = 2I_2$ and $Q_u = 0.1$ for each data point. Once the training dataset $\mathbb{D}_{training}$ is generated, we use PyTorch package [57] and Adam optimizer [58] to train a feedforward NN with 6 hidden layers, and with 8, 32, 64, 64, 32, and 16 neurons in the hidden layers; note that the training converges within 10000 epochs given a learning rate of 0.001. Finally, we implement the resulting NN-based control scheme on Python 3.10.

6.1. Determining the RoA

We use the method described in Subsection 5.2 to determine the RoA for $r = 0$ and with different values of θ . More precisely, we divided the operating region \mathcal{X} into 10^6 grid cells, and used the developed NN-based control to compute simulated trajectory with the initial condition being equal to each cell; the initial condition belongs to the RoA if the trajectory remains entirely inside the operating region \mathcal{X} . The obtained RoA with $\theta = 0.01$ is shown in Figure5. Note that the obtained RoA $\Phi(0)$ with $\theta = 0.001$ and $\theta = 0.0001$ are almost the same as for $\theta = 0.01$, and thus are not presented.

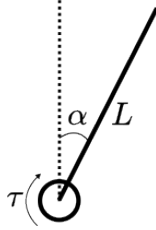


Figure 4: Inverted pendulum system.

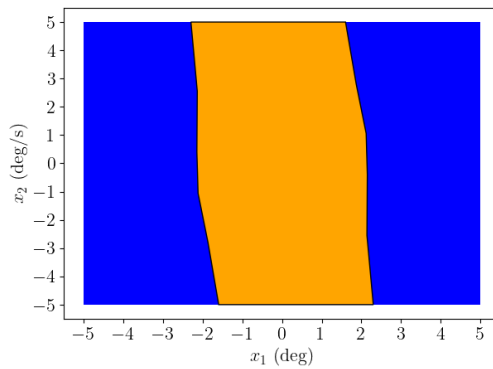


Figure 5: The obtained RoA with $\theta = 0.01$ and $r = 0$; the blue and yellow represent \mathcal{X} and $\Phi(0)$, respectively.

6.2. Performance Analysis

To evaluate the effectiveness of the proposed one-step-ahead predictive control scheme and the NN-based control scheme, we consider three cases based on the choice of the parameter θ . To provide a quantitative comparison, we consider 1,000 experiments with $r = 0$ and with the initial condition $x(0) = [x_1(0) \ x_2(0)]^\top$, where in each experiment, $x_1(0)$ and $x_2(0)$ are uniformly selected from the interval $[-1, 1]$, which belongs to the RoA shown in Figure 5; note that the same initial condition is applied to all cases to ensure a fair comparison.

The obtained results are reported in Table 1, where Performance Index (PI) is defined as $PI = \sum \|x(t)\|$. As seen in this table, using a large θ can improve the performance with both one-step-ahead predictive control scheme and the NN-based control scheme, even though the improvement with the NN-based control scheme is more significant than that with the one-step-ahead predictive control scheme.

Table 1 reveals that for $\theta = 0.01$ and $\theta = 0.001$, the NN-based control scheme provides a better tracking performance compared to the one-step-ahead predictive control scheme. Note that this is understandable, as the one-step-ahead predictive control scheme is tailored to minimize the cost function given in (3a), which is different than the considered metric for comparing the tracking performance.

Figure 6 represents a typical time profile of the system states with NN-based control scheme and one-step-ahead predictive control scheme for $\theta = 0.0001$. As seen in this figure, the tracking error with the NN-based control is greater than that of the one-step-ahead-predictive control.

Table 1: Performance Index for Different Values of θ and Different Control Methods.

Performance Index [deg]	One-Step-Ahead Predictive Control	NN-Based Control
$\theta = 0.0100$	8.454	6.430
$\theta = 0.0010$	8.495	7.047
$\theta = 0.0001$	8.513	11.998

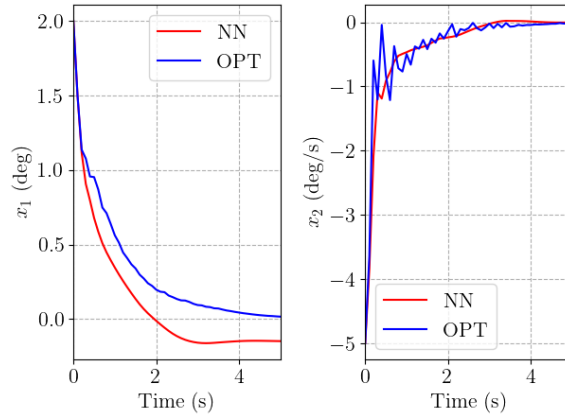


Figure 6: Time profile of $x(t)$ with $\theta = 0.0001$.

Note that NN-based control scheme is faster than the one-step-ahead control scheme, and thus is appropriate for real-time applications. For instance, when $\theta = 0.01$, the mean computing time for the NN-based control scheme is 0.565 seconds, while the mean computing time for the one-step-ahead predictive controls scheme is 180.551 seconds; that is the NN-based control scheme is 319 times faster than the one-step-ahead predictive control scheme.

6.3. Time-Domain Analysis

This section provides time-domain results of the proposed NN-based control scheme. We present results with $\theta = 0.01$, $\theta = 0.001$, and $\theta = 0.0001$ for $r = 0$. For comparison purposes, we also consider the iterative LQR technique, where the dynamics of the inverted pendulum is linearized at every time instant, and then an infinite-horizon LQR control law is computed for the linearized system. The initial condition is $x(0) = [-2.3 \ 5]^T$; note that according to Figure 5, it is obvious that $x(0) \in \Phi(0)$.

Figure 7 shows the time profile of the state variables $x_1(t)$ and $x_2(t)$, and the control input $u(t)$. As seen in this figure, the proposed NN-based control scheme can effectively steer the angle of the inverted pendulum to zero. It should be noted that as expected, the larger the value of θ is, the better the tracking performance can become. In particular, the PI index defined above is 26.37, 26.99, and 31.17 with $\theta = 0.01$, $\theta = 0.001$, and $\theta = 0.0001$, respectively. Similar to the extensive simulation studies reported in Subsection 6.2, $\theta = 0.01$ and $\theta = 0.001$ provide a comparable tracking performance, while $\theta = 0.0001$ significantly degrades the tracking performance.

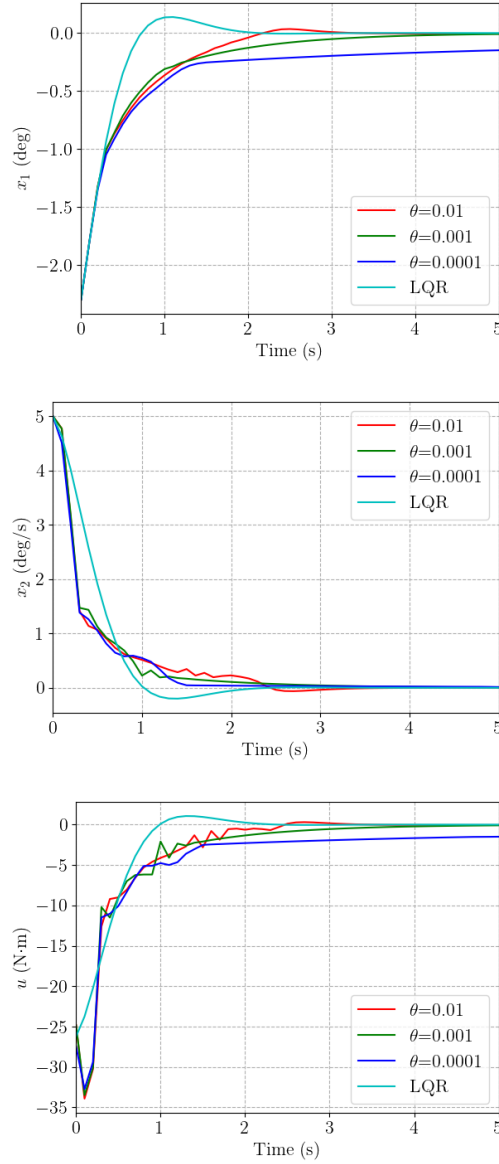


Figure 7: Time profile of state vector $x(t)$ and control input $u(t)$.

Also, Figure7 reveals that the iterative LQR technique provides a better solution in comparison with the proposed NN-based control scheme; note that this observation is understandable, as the linearization error δ discussed in Assumption 2 is small throughout the RoA $\Phi(0)$.

Phase portrait of the system is shown in Figure8, where the arrows show the moving direction of states. Note that the length of each arrow shows the speed of movement; that is, the higher the length of the arrow is, the faster the states move.

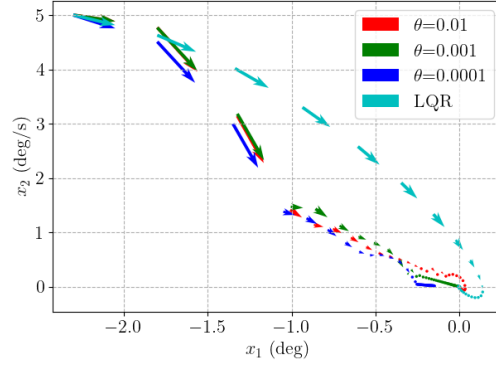


Figure 8: Phase portrait graph.

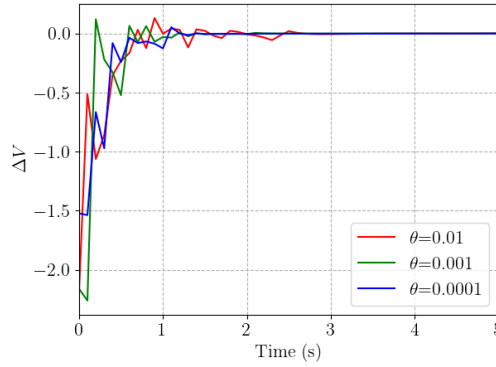


Figure 9: Time profile of $\Delta V(t)$.

Figure 9 shows the time profile of $\Delta V(t)$ defined in (5). As seen in this figure, when the state vector $x(t)$ is far away from the equilibrium point (i.e., the origin), $\Delta V(t)$ is negative implying that the Lyapunov function is decreasing. As $x(t)$ gets closer to the equilibrium point, due to training errors, $\Delta V(t)$ may take positive values. Nevertheless, as mentioned in Theorem 3, the system is stable and the tracking error remains bounded.

7. Experimental Results

To validate the proposed scheme in practical scenarios, we employ it to control the position of a Parrot Bebop 2 drone. The dynamical model of the drone can be expressed as [59]:

$$\dot{x} = \begin{bmatrix} 0 & 1 & 0 & 0 & 0 & 0 \\ 0 & -0.0527 & 0 & 0 & 0 & 0 \\ 0 & 0 & 0 & 1 & 0 & 0 \\ 0 & 0 & 0 & -0.0187 & 0 & 0 \\ 0 & 0 & 0 & 0 & 0 & 1 \\ 0 & 0 & 0 & 0 & 0 & -1.7873 \end{bmatrix} x + \begin{bmatrix} 0 & 0 & 0 \\ -5.4779 & 0 & 0 \\ 0 & 0 & 0 \\ 0 & -7.0608 & 0 \\ 0 & 0 & 0 \\ 0 & 0 & -1.7382 \end{bmatrix} u,$$

$$y = \begin{bmatrix} 1 & 0 & 0 & 0 & 0 & 0 \\ 0 & 0 & 1 & 0 & 0 & 0 \\ 0 & 0 & 0 & 0 & 1 & 0 \end{bmatrix} x,$$

It should be noted that the dynamics along X, Y, and Z directions are decoupled; thus, we employed identical structured NN models in all three directions. More precisely, three feedforward NNs are utilized, each with 6 hidden layers, and 8, 32, 64, 64, 32, and 16 neurons in the hidden layers.

To collect the dataset, for the X and Y directions, we set $\mathcal{X} = [-0.5, 0.5] \times [-1, 1]$ and $\mathcal{R} = [0, 0]$. For the Z direction, we set $\mathcal{X} = [1, 2] \times [-1, 1]$ and $\mathcal{R} = [1.5, 0]$. The training dataset, denoted as $\mathbb{D}_{\text{training}}$, is generated by gridding the aforementioned regions with steps of 0.01; thus, $|\mathbb{D}_{\text{training}}| = 40404$ for each direction.

We utilize the YALMIP toolbox to solve the optimization problem (3) for each data point, where $Q_x = 20I_2$ and $Q_u = 0.1$. We set $\theta = 1$ for all scenarios. After collecting the data, we used the same training parameters and strategies as those used for the inverted pendulum system within 10000 epochs. Subsequently, the models are trained and converted into executable MATLAB format.

We compared the trained NN models with the LQR control method. To ensure a fair comparison, we set the weighting matrices of the LQR to be the same as the weighting matrices in the optimization problem (3).

Figure 10 presents the time profile of the drone's position. Also, control effort defined as $\sum |u(t)|$ for the proposed method and LQR is reported in Table 2. As seen in Figure 10, for the X and Y directions, our NN models outperformed the LQR method, as the linearization error in these directions is large; while the LQR method provided relatively better results in the Z direction. This observation is reasonable, as the optimization problem (3) is different that underlying optimization problem in LQR framework.

8. Conclusion

This paper proposed a systematic and comprehensive methodology to design provably-stable NN-based control schemes for affine nonlinear systems. First, a novel one-step-ahead predictive control method was developed; its stability and convergence properties were analytically proven. Then, an approach was presented to train a NN that imitates the behavior of the one-step-ahead predictive control scheme in a given operating region. Stability and convergence properties of

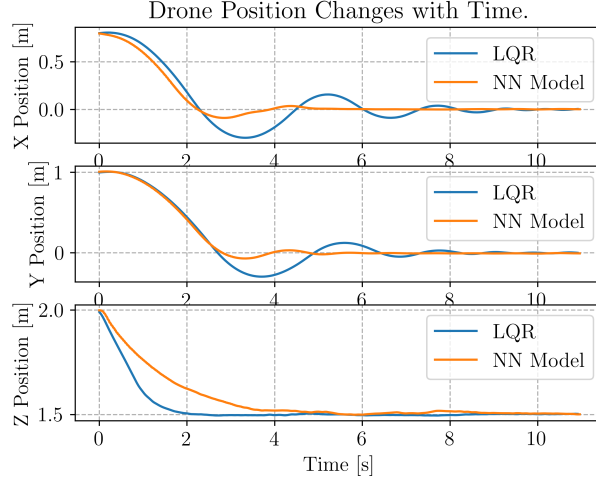


Figure 10: Time profile of the drone's position.

Table 2: Control effort (i.e., $\sum |u(t)|$) with NN models and LQR in three directions.

Direction	X	Y	Z
Proposed Method	33.3	29.6	65.6
LQR	61.7	59.8	95.9

the closed-loop system with the trained NN in the loop were shown via rigorous analysis. In particular, it was shown that the resulting NN-based control scheme guarantees that the states of the system remain bounded, and asymptotically converge to a neighborhood around the desired equilibrium point, with a tunable proximity threshold. The effectiveness of the proposed approach was assessed via extensive simulation and experimental studies.

The main limitation of the proposed method is that the optimization problem (3) is nonlinear and non-convex with respect to decision variables u and P , and existing solvers may not be able to solve its all instances for any given system. Thus, the NN trained on the dataset obtained by numerically solving the optimization problem (3) may give a large approximation error (i.e., large Δu and ΔP), and thus according to (28), the resulting NN-based control scheme may yield poor performance. Future work will investigate methods to effectively solve the optimization problem (3) and collect a decent training dataset.

Data Availability

All the code and data used in simulation and experimental studies are available at <https://github.com/anran-github/Provably-Stable-Neural-Network-Based-Control-of-Nonlinear-Systems.git>.

References

- [1] H. K. Khalil, *Nonlinear Systems*. Upper Saddle River, NJ, USA: Prentice Hall, 2002.

- [2] A. Isidori, *Nonlinear Control Systems*. London: Springer Verlag, 1995.
- [3] K. Ogata, *Modern Control Engineering*. Prentice Hall, 2010.
- [4] C.-T. Chen, *Linear System Theory and Design*. Oxford University Press, 1998.
- [5] W. Li and E. Todorov, "Iterative linear quadratic regulator design for nonlinear biological movement systems," in *Proc. 1st International Conference on Informatics in Control, Automation and Robotics*, 2004, pp. 222–229.
- [6] E. Todorov and W. Li, "A generalized iterative LQG method for locally-optimal feedback control of constrained nonlinear stochastic systems," in *Proc. American Control Conference*, Portland, OR, USA, Jun. 8–10, 2005, pp. 300–306.
- [7] C. R. Rodrigues, R. Kuiava, and R. A. Ramos, "Design of a linear quadratic regulator for nonlinear systems modeled via norm-bounded linear differential inclusions," *IFAC Proceedings Volumes*, vol. 44, no. 1, pp. 7352–7357, Jan. 2011.
- [8] L. B. Prasad, B. Tyagi, and H. O. Gupta, "Optimal control of nonlinear inverted pendulum system using PID controller and LQR: Performance analysis without and with disturbance input," *International Journal of Automation and Computing*, vol. 11, pp. 661–670, 2014.
- [9] R. I. Bobby, H. Mansor, T. S. Gunawan, and S. Khan, "Robust adaptive LQR control of nonlinear system application to 3-Dof flight control system," in *Proc. IEEE International Conference on Smart Instrumentation, Measurement and Applications*, Kuala Lumpur, Malaysia, Nov. 25, 2014.
- [10] K. Mathiyalagan and G. Sangeetha, "Finite-time stabilization of nonlinear time delay systems using LQR based sliding mode control," *Journal of the Franklin Institute*, vol. 356, no. 7, pp. 3948–3964, May 2019.
- [11] J. Chen, W. Zhan, and M. Tomizuka, "Constrained iterative LQR for on-road autonomous driving motion planning," in *Proc. IEEE 20th International Conference on Intelligent Transportation Systems*, Yokohama, Japan, Oct. 16–19, 2017, pp. 1–7.
- [12] S. Sastry, *Nonlinear Systems: Analysis, Stability, and Control*. Springer New York, NY, 1999.
- [13] J. B. Rawlings, E. S. Meadows, and K. R. Muske, "Nonlinear model predictive control: A tutorial and survey," *IFAC Proceedings Volumes*, vol. 27, no. 2, pp. 185–197, May 1994.
- [14] M. Vidyasagar, *Nonlinear Systems Analysis*. Prentice Hall, 1993.
- [15] K. J. Hunt, G. R. Irwin, and K. Warwick, *Neural Network Engineering in Dynamic Control Systems*. Springer London, 1995.
- [16] R. Sinha, J. Harrison, S. M. Richards, and M. Pavone, "Adaptive robust model predictive control with matched and unmatched uncertainty," in *Proc. American Control Conference*, Atlanta, GA, USA, Jun. 8–10, 2021, pp. 906–913.
- [17] O. Elhaki and K. Shojaei, "A robust neural network approximation-based prescribed performance output-feedback controller for autonomous underwater vehicles with actuators saturation," *Engineering Applications of Artificial Intelligence*, vol. 88, p. 103382, 2020.
- [18] Z. Cheng, H. Pei, and S. Li, "Neural-networks control for hover to high-speed-level-flight transition of ducted fan uav with provable stability," *IEEE Access*, vol. 8, pp. 100 135–100 151, 2020.
- [19] J. Zhou, H. Xu, Z. Li, S. Shen, and F. Zhang, "Control of a tail-sitter VTOL UAV based on recurrent neural networks," *arXiv preprint arXiv:2104.02108*, 2021.
- [20] F. Jiang, F. Pourpanah, and Q. Hao, "Design, implementation, and evaluation of a neural-network-based quadcopter UAV system," *IEEE Transactions on Industrial Electronics*, vol. 67, no. 3, pp. 2076–2085, 2019.
- [21] X. Li, M. Jusup, Z. Wang, H. Li, L. Shi, B. Podobnik, and H. Stanley, S. Havlin, and S. Boccaletti, "Punishment diminishes the benefits of network reciprocity in social dilemma experiments," *Proceedings of the National Academy of Sciences*, vol. 115, pp. 20–35, Feb. 2018.
- [22] H. Dai, B. Landry, L. Yang, M. Pavone, and R. Tedrake, "Lyapunov-stable neural-network control," *arXiv preprint arXiv:2109.14152*, 2021.
- [23] D. Grande, A. Peruffo, E. Anderlini, and G. Salavasidis, "Augmented neural Lyapunov control," *IEEE Access*, vol. 11, pp. 67 979–67 986, 2023.
- [24] H. V. Nghi, D. Phuoc Nhien, N. T. Minh Nguyet, N. Tu Duc, N. P. Luu, P. Son Thanh, L. T. Hong Lam, and D. Xuan Ba, "A LQR-based neural-network controller for fast stabilizing rotary inverted pendulum," in *Proc. International Conference on System Science and Engineering*, Ho Chi Minh City, Vietnam, Aug. 26–28, 2021, pp. 19–22.
- [25] F. W. Alsaade, H. Jahanshahi, Q. Yao, M. S. Al-zahrani, and A. S. Alzahrani, "A new neural network-based optimal mixed H_2/H_∞ control for a modified unmanned aerial vehicle subject to control input constraints," *Advances in Space Research*, vol. 71, no. 9, pp. 3631–3643, 2023.
- [26] R. C. Rego and F. M. U. de Araujo, "Lyapunov-based continuous-time nonlinear control using deep neural network applied to underactuated systems," *Engineering Applications of Artificial Intelligence*, vol. 107, p. 104519, 2022.
- [27] K. Esfandiari, F. Abdollahi, and H. A. Talebi, *Neural Network-Based Adaptive Control of Uncertain Nonlinear Systems*. Springer, Cham, 2021.
- [28] M. Jang, J. Hyun, T. Kwag, C. Gwak, C. Jeong, T. A. Nguyen, and J.-W. Lee, "es-DNLC: A deep neural network control with exponentially stabilizing control lyapunov functions for attitude stabilization of PAV," in *Proc. 22nd*

- International Conference on Control, Automation and Systems*, 2022, pp. 81–86.
- [29] M. Jang, J. Hyun, T. Kwag, C. Gwak, T. A. Nguyen, and J.-W. Lee, “UAMDynCon-DT: A data-driven dynamics and robust control framework for UAM vehicle digitalization using deep learning,” in *Proc. International Conference on Mechatronics, Control and Robotics*, 2023, pp. 81–85.
- [30] P. L. Donti, M. Roderick, M. Fazlyab, and J. Z. Kolter, “Enforcing robust control guarantees within neural network policies,” *arXiv preprint arXiv:2011.08105*, 2020.
- [31] J. Autenrieb, H.-S. Shin, and M. Bacic, “Development of a neural network-based adaptive nonlinear dynamic inversion controller for a tilt-wing VTOL aircraft,” in *Proc. Workshop on Research, Education and Development of Unmanned Aerial Systems*, 2019, pp. 44–52.
- [32] H. Ravanbakhsh and S. Sankaranarayanan, “Learning control lyapunov functions from counterexamples and demonstrations,” *Autonomous Robots*, vol. 43, pp. 275–307, 2019.
- [33] E. F. Camacho, C. Bordons, E. F. Camacho, and C. Bordons, *Model predictive controllers*. Springer, 2007.
- [34] J. B. Rawlings, D. Q. Mayne, and M. Diehl, *Model predictive control: theory, computation, and design*. Nob Hill Publishing Madison, WI, 2017, vol. 2.
- [35] L. Grune and J. Pannek, *Nonlinear Model Predictive Control: Theory and Algorithms*. Springer-Verlag London, 2011.
- [36] F. Allgower and A. Zheng, *Nonlinear Model Predictive Control*. Springer Science & Business Media, 2000.
- [37] M. Hosseinzadeh, B. Sinopoli, I. Kolmanovsky, and S. Baruah, “Robust to early termination model predictive control,” *IEEE Transactions on Automatic Control*, 2023, DOI: 10.1109/TAC.2023.3308817.
- [38] X. Yin, A. Jindal, V. Sekar, and B. Sinopoli, “A control-theoretic approach for dynamic adaptive video streaming over HTTP,” in *Proc. ACM Conf. Special Interest Group on Data Communication*, London, United Kingdom, Aug. 17–21, 2015, pp. 325–338.
- [39] M. Hosseinzadeh, K. Shankar, M. A. abd Jay Ramachandran, S. Adams, V. Sekar, and B. Sinopoli, “CANE: A cascade-control approach for network-assisted video QoE management,” *IEEE Transactions on Control Systems Technology*, vol. 31, no. 6, pp. 2543–2554, Nov. 2023.
- [40] C. Kambhampati, J. D. Mason, and K. Warwick, “A stable one-step-ahead predictive control of non-linear systems,” *Automaticas*, vol. 36, no. 4, pp. 485–495, Apr. 2000.
- [41] V. C. Aitken and H. M. Schwartz, “On the exponential stability of discrete-time systems with applications in observer design,” *IEEE Transactions on Automatic Control*, vol. 39, no. 9, pp. 1959–1962, Sep. 1994.
- [42] T. L. Fine, *Feedforward Neural Network Methodology*. Springer New York, NY, 1999.
- [43] I. Goodfellow, Y. Bengio, and A. Courville, *Deep Learning*. MIT Press, 2016.
- [44] U. Evci, B. van Merriënboer, T. Unterthiner, F. Pedregosa, and M. Vladymyrov, “GradMax: Growing neural networks using gradient information,” in *Proc. 10th International Conference on Learning Representations*, Apr. 25–29, 2022.
- [45] L. Wu, B. Liu, P. Stone, and Q. Liu, “Firefly neural architecture descent: a general approach for growing neural networks,” in *Proceedings of the Advances in Neural Information Processing Systems 33*, Dec. 6–12, 2020.
- [46] Y. Bengio, N. Roux, P. Vincent, O. Delalleau, and P. Marcotte, “Convex neural networks,” in *Proc. Advances in Neural Information Processing Systems*, Vancouver, BC, Canada, 2005.
- [47] N. Srivastava, G. Hinton, A. Krizhevsky, I. Sutskever, and R. Salakhutdinov, “Dropout: a simple way to prevent neural networks from overfitting,” *The journal of machine learning research*, vol. 15, no. 56, pp. 1929–1958, 2014.
- [48] H.-i. Lim, “A study on dropout techniques to reduce overfitting in deep neural networks,” in *Proc. 14th International Conference on Multimedia and Ubiquitous Engineering*, Jeju, South Korea, Aug. 17–19, 2020, pp. 133–139.
- [49] K. Sanjar, A. Rehman, A. Paul, and K. JeongHong, “Weight dropout for preventing neural networks from overfitting,” in *Proc. 8th International conference on orange technology*, Daegu, Korea (South), Dec. 18–21, 2020.
- [50] H. Wu and X. Gu, “Towards dropout training for convolutional neural networks,” *Neural Networks*, vol. 71, pp. 1–10, Nov. 2015.
- [51] Z. Liu, “Super convergence cosine annealing with warm-up learning rate,” in *Proc. 2nd International Conference on Artificial Intelligence, Big Data and Algorithms*, Nanjing, China, Jun. 17–19, 2022, pp. 768–774.
- [52] J. K. Eshraghian, C. Lammie, M. R. Azghadi, and W. D. Lu, “Navigating local minima in quantized spiking neural networks,” in *Proc. IEEE 4th International Conference on Artificial Intelligence Circuits and Systems*, Incheon, Korea, Republic of, Jun. 13–15, 2022, pp. 352–355.
- [53] D. F. Watson, “Computing the n -dimensional delaunay tessellation with application to voronoi polytopes,” *The Computer Journal*, vol. 24, no. 2, pp. 167–172, 1981.
- [54] C. L. Lawson, “Properties of n -dimensional triangulations,” *Computer Aided Geometric Design*, vol. 3, no. 4, pp. 231–246, Dec. 1986.
- [55] O. Boubaker, “The inverted pendulum benchmark in nonlinear control theory: a survey,” *International Journal of Advanced Robotic Systems*, vol. 10, no. 5, 2013.
- [56] J. Lofberg, “YALMIP: a toolbox for modeling and optimization in MATLAB,” in *Proc. IEEE International Conference on Robotics and Automation*, Taipei, Taiwan, Sep. 2–4, 2004, pp. 284–289.

- [57] <https://pytorch.org>, [Accessed February 4, 2025].
- [58] D. P. Kingma and J. Ba, "Adam: A method for stochastic optimization," *arXiv preprint arXiv:1412.6980v9*, 2017.
- [59] M. Amiri and M. Hosseinzadeh, "Closed-loop model identification and MPC-based navigation of quadcopters: A case study of parrot bebop 2," *arXiv:2404.07267*, 2024. [Online]. Available: <https://arxiv.org/abs/2404.07267>